



**Report 201915 - 19-DB-21**

**Luc Jaouen, François-Xavier Bécot, Fabien Chevillotte**

**Update: October 30, 2019**

**On request of  
dBVibroacoustics s.r.o.  
Husinecka 903/10, 130 00,  
Praha 3,  
Czech Republic**



**Following purchase order 20190517-1P signed on May the 17th of 2019.**

## Contents

<b>I Results</b>	<b>3</b>
<b>1 DB 21</b>	<b>3</b>
1.1 Static air-flow resistivity . . . . .	3
1.2 Open porosity . . . . .	4
1.3 Tortuosity, characteristic lengths and static thermal permeability . . . . .	4
1.4 Elastic parameters . . . . .	5
<b>2 Measuring the thickness of samples</b>	<b>7</b>
<b>3 Estimating the acoustical parameters</b>	<b>7</b>
<b>4 Estimating the elastic and damping parameters</b>	<b>8</b>

### MATELYS - RESEARCH LAB

Ltd liability company with total share 8250 euros – *Agrément C.I.R. (Crédit Impôt Recherche) since 2007*  
*Organisme de formation : Déclaration d'activité enregistrée n° 82691051869 auprès du préfet de région*  
SIRET 487 596 009 00034 – TVA EU FR 06 487 596 009

Head office: 7 rue des Maraîchers, Bâtiment B, 69120 Vaulx-en-Velin – France  
Phone: +33 9 72 50 93 16 – Fax : +33 9 72 50 93 15  
<http://www.matelys.com> – [contact@matelys.com](mailto:contact@matelys.com)

# Part I

## Results

### 1 DB 21

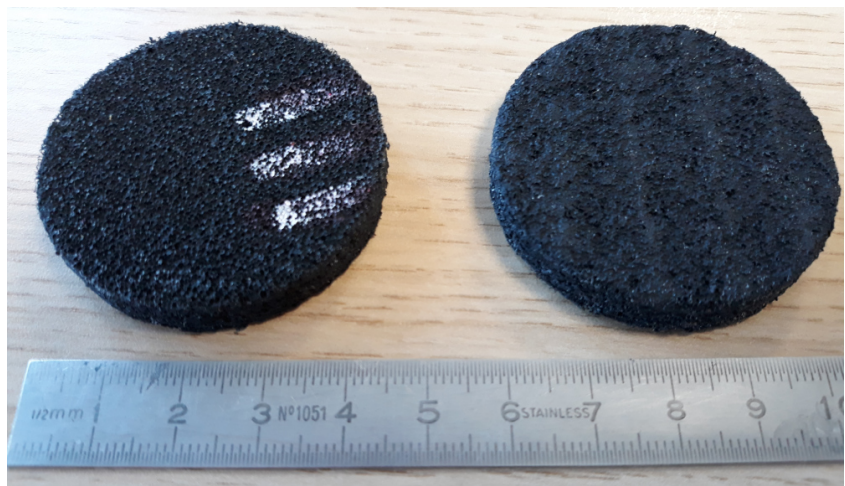


Figure 1: **DB 21** : Picture of two material samples after tests. On the left, the visible face is named “a”. On the right, the visible face is named “b”. Face a shows a uniform granular black surface while face b shows some clearer stripes and a more dense surface. The two faces exhibits different properties (i.e. the material is heterogenous). The results below concern face a (which is assumed to be the face toward sound incidence).

#### 1.1 Static air-flow resistivity

The static air flow resistivity of the material has been estimated using the low asymptote approach as described in the appendix of ISO 9053-1:2018<sup>1</sup>.  $\delta\sigma$  represents the standard deviation of each estimation for a given sample.

Test	$\sigma$ ( $\delta\sigma$ )	Thickness
21 i a	168 400 (13 400)	8.0
21 ii a	203 100 (15 100)	8.1
21 iii a	152 100 (11 800)	7.9
Mean values ( $\sigma_X$ )	174 500 (26 000)	8.0 (0.1)
Units	N.s.m <sup>-4</sup>	mm

Table 1: **DB 12 - face a**: Measurement results for the static air flow resistivity. Values for each tested sample, mean value and standard deviation ( $\sigma_X$ ) over all samples.

The relative standard deviation of these static air-flow resistivities measurements is 14%. This result indicates a significant heterogeneity between the tested samples.

<sup>1</sup> ISO 9053-1. Acoustics – determination of airflow resistance – part 1: Static air-flow method. *International Organization for Standardization*, 2018.

## 1.2 Open porosity

The value of the open porosity has been estimated using the low asymptote approach as described in Jaouen et al. 2018<sup>2</sup>.  $\delta\sigma$  represents the standard deviation of each estimation for a given sample.

Test	$\phi$ ( $\delta$ )
21 i a	0.49 (0.11)
21 ii a	0.51 (0.10)
21 iii a	0.48 (0.10)
<b>Mean value</b> ( $\sigma_X$ )	<b>0.49</b> (0.02)
Unit	

<sup>2</sup> L. Jaouen, E. Gourdon, and M. Edwards. 6-parameter acoustical characterization of porous media using a classical impedance tube. In *Proc. of Euronoise 2018 (27-31 May, Hersonissos, Crete, Greece)*, 2018.

Table 2: **DB 12 - face a**: Measurements results for the open porosity. Values for each test, mean value and standard deviation ( $\sigma_X$ ) over all tests.

The relative standard deviation is 4%, however the precision of the method for such mean value is 10%.

## 1.3 Tortuosity, characteristic lengths and static thermal permeability

Estimations of the high frequency limit of the dynamic tortuosity, the characteristic viscous and thermal lengths and the static thermal permeability of the material have been realised from measured data of dynamic mass densities and compressibilities (see section 3).

Test	$\alpha_\infty$ ( $\delta$ )	$\Lambda$ ( $\delta$ )	$\Lambda'$ ( $\delta$ )	$k'_0$ ( $\delta$ )	Thickness
21 i a	1.41 (0.39)	4 (0)	217 (44)	10 (2)	8.0
21 ii a	1.43 (0.48)	4 (0)	280 (34)	21 (69)	8.1
21 iii a	1.36 (0.76)	4 (0)	219 (16)	10 (1)	7.9
<b>Mean values</b> ( $\sigma_X$ )	<b>1.4</b> (0.54)	<b>4</b> (0)	<b>238</b> (48)	<b>14</b> (25)	<b>8.0</b> (0.1)
Units		$\mu\text{m}$	$\mu\text{m}$	$10^{-10}\text{m}^2$	mm

Table 3: **DB 12 - face a**: Estimation of the acoustic parameters of the Johnson-Champoux-Allard-Lafarge model. Values for each tested sample, mean value and standard deviation ( $\sigma_X$ ) over all samples.

### 1.3.1 Validation of the parameters

Figure 2 compares the sound absorption coefficient as measured in the impedance tube and as computed using a Johnson-Champoux-Allard-Lafarge model (JCAL) according to the mean values of the parameters characterized above (i.e. or face a).

Measured data are represented as the dispersion envelope obtained over all characterized samples.

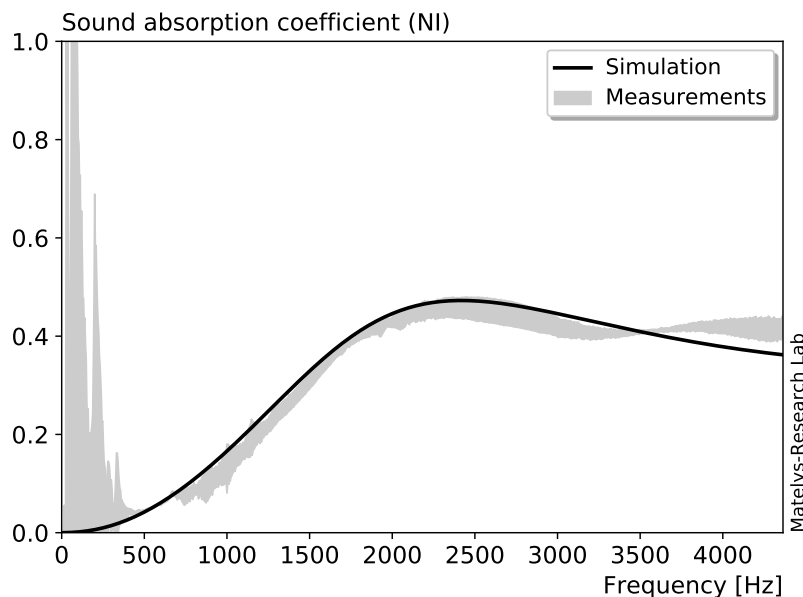


Figure 2: **DB 12 - face a** : sound absorption coefficient for plane waves under normal incidence (NI).  
■ : dispersion over measured samples,  
— : simulation using the JCAL model,  
Material backed with an impervious and rigid backing.  
Temperature : 23°C  
Ambiant pressure: 101 400 Pa  
Hygrometry: 42%

As a comparison, Figure 3 compares the sound absorption coefficient as measured in the impedance tube and as computed using a Johnson-Champoux-Allard-Lafarge model (JCAL) for the opposite face : face b. Another set of parameters was used to draw the simulation curve in black.

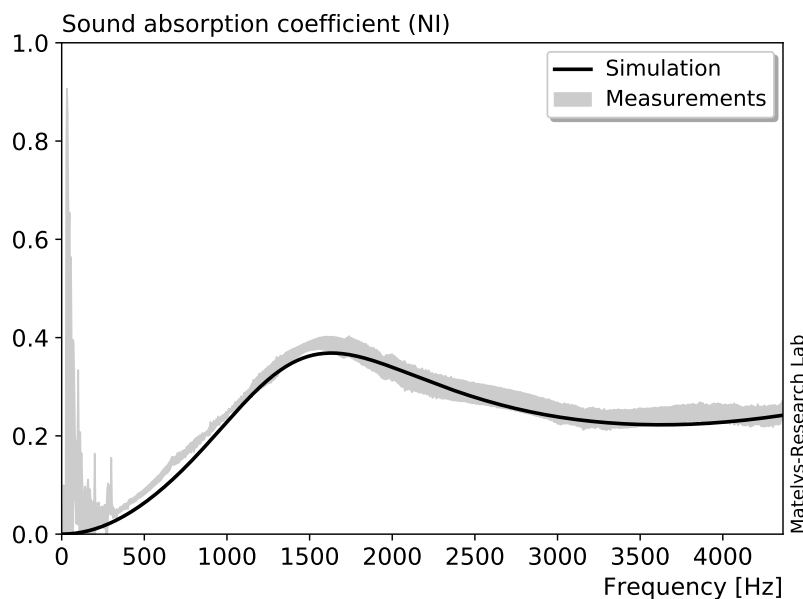


Figure 3: **DB 12 - face b** : sound absorption coefficient for plane waves under normal incidence (NI).  
■ : dispersion over measured samples,  
— : simulation using the JCAL model,  
Material backed with an impervious and rigid backing.  
Temperature : 23°C  
Ambiant pressure: 101 400 Pa  
Hygrometry: 42%

### 1.4 Elastic parameters

The following table presents the elastic characterization results for samples of the material under an uni-axial compression test (see section 4).

Note that, from an elastic point of view, no noticeable difference was measured between face a and face b of the material samples<sup>3</sup>.

<sup>3</sup> Or the heterogeneity between faces was lower than the measurement uncertainties.

<i>Test</i>	<b>E</b>	<i><math>\eta</math></i>	<i><math>\nu</math></i>	<i><math>\rho</math></i>
<i>1</i>	11 854.1	0.42	0.34	1 042
<i>2</i>	11 657.7	0.45	0.36	1 037
<i>3</i>	12 124.8	0.45	0.39	1 051
<b>Mean values</b> ( $\sigma_X$ )	<b>11 878.9</b> (234.5)	<b>0.44</b> (0.02)	<b>0.36</b> (0.03)	<b>1 043</b> (7)
Units	$\times 10^3 \text{ N.m}^{-2}$			$\text{kg.m}^{-3}$

*Conditions:*

Temperature: 23 °C                      Static stress  $\sim$  2332 Pa  
Ambiant Pressure: 101 400 Pa      Resonance freq.  $\in$  [150 - 250] Hz  
Hygrometry : 42%

Table 4: **DB 12** : elastic and damping parameters of the tested material assumed to be isotropic. Values for each tested sample, mean value and standard deviation ( $\sigma_X$ ) over all samples.

## 2 Measuring the thickness of samples

The thicknesses of material samples are manually measured using an electronic calipers with a precision of 0.01 mm. for material samples which do not have a perfect flat surface, the thickness precision is 0.1 mm.

## 3 Estimating the acoustical parameters

Regarding the acoustic characterisation of a material, the parameters are estimated from acoustic measurements obtained in a stationary wave tube.

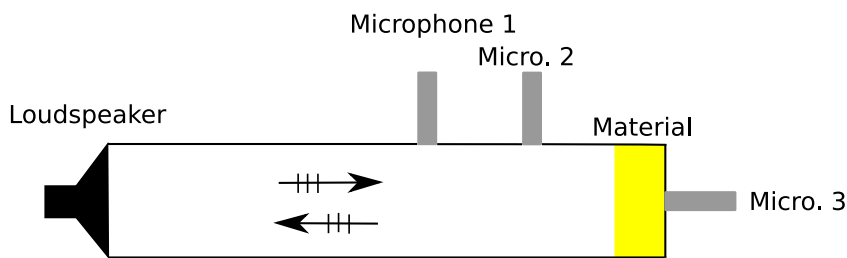


Figure 4: Scheme of the experimental setup used for the measurement of the dynamic volumic mass and compressibility. This setup is used for the estimation of all the acoustic parameters.

The measured values of the acoustic pressure in front of and at the rear of the sample, as a function of frequency, are used to determine the dynamic volumic mass and compressibility of the sample (see fig. 4).

The static air flow resistivity  $\sigma$  is estimated from the imaginary part of the dynamic mass density as described in the appendix section of ISO 9053-1:2018<sup>4</sup>.

The open porosity  $\phi$  is estimated from the real part of the dynamic bulk modulus as described in Jaouen et al.<sup>5</sup>

<sup>4</sup> ISO 9053-1. Acoustics – determination of airflow resistance – part 1: Static airflow method. *International Organization for Standardization*, 2018.

<sup>5</sup> L. Jaouen, E. Gourdon, and M. Edwards. 6-parameter acoustical characterization of porous media using a classical impedance tube. In *Proc. of Euronoise 2018 (27-31 May, Hersonissos, Crete, Greece)*, 2018.

The parameters  $\alpha_\infty$ ,  $\Lambda$  and  $\Lambda'$  are then estimated from their analytical expressions<sup>6,7</sup> which are deduced from the Johnson-Champoux-Allard (JCA) model<sup>8,9</sup> or the Johnson-Champoux-Allard-Lafarge (JCAL) model<sup>10</sup>. One may note that these models assume that the porous material has a rigid and motionless skeleton.

Finally, at most, the acoustic parameters which are determined in the direction normal to the material surface are:

- the static air flow resistivity  $\sigma$  ( $\text{N.s.m}^{-4}$ ),
- the open porosity  $\phi$ ,
- the high frequency limit of the dynamic tortuosity  $\alpha_\infty$ ,
- the viscous characteristic length  $\Lambda$  (m),
- the thermal characteristic length  $\Lambda'$  (m),
- the static thermal permeability  $k'_0$  ( $\text{m}^2$ ).

The possible situations where the material exhibits a “limp” behaviour<sup>11</sup> is handled as previously described using an adapted model. If the material exhibits resonances associated to the deformation of the porous skeleton, the frequency ranges where this phenomenon occurs are omitted when characterising the material.

#### 4 Estimating the elastic and damping parameters

The method used in this report is based on the study of the vibrations of a mass – spring system under an uni-axial compression test.

The measured Frequency Response Function (FRF) is defined as the ratio of the displacements of the top rigid mass to the base moving plate for a rectangular parallelepiped or cylindrical (with circular cross section) sample material (see Fig. 5). From a practical point of view, an accelerometer is used to determine the base plate displacement and a second one is used to determine the displacement of the top loading mass.

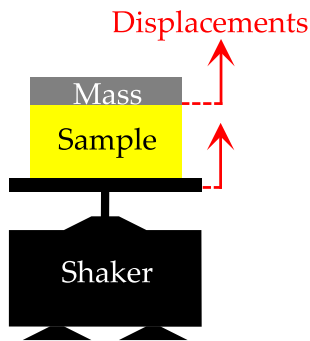


Figure 5: Scheme of the experimental setup used in the mass – spring resonance method.

This method can be used for the determination of the Young's modulus, the Poisson coefficient and the structural loss factor of an assumed isotropic material sample when the top loading mass is known. The analysis of the FRF in the vicinity of the resonance of the mass-spring system allows to determine the structural loss factor and the apparent Young's modulus. This latter modulus is linked to the actual Young's modulus of the material by a factor which depends on the shape of the sample and on the Poisson's ratio of the material. Thus, for a given shape factor<sup>12</sup>, this coefficient only depends on the Poisson's ratio of the material<sup>13</sup>. Therefore, by testing samples having different shape factors, the Poisson's ratio can be estimated. Finally, from this latter value, the actual Young's modulus of the material can be determined.

<sup>6</sup> R. Panneton and X. Olny. Acoustical determination of the parameters governing viscous dissipation in porous media. *J. Acoust. Soc. Am.*, 119:2027–2040, 2006.

<sup>7</sup> X. Olny and R. Panneton. Acoustical determination of the parameters governing thermal dissipation in porous media. *J. Acoust. Soc. Am.*, 123:814–824, 2008.

<sup>8</sup> D. L. Johnson, J. Koplik, and R. Dashen. Theory of dynamic permeability and tortuosity in fluid-saturated porous media. *J. Fluid Mech.*, 176:379–402, 1987.

<sup>9</sup> Y. Champoux and J.-F. Allard. Dynamic tortuosity and bulk modulus in air-saturated porous media. *J. Appl. Phys.*, 70:1975–1979, 1991.

<sup>10</sup> D. Lafarge, P. Lemarinier, J.-F. Allard, and V. Tarnow. Dynamic compressibility of air in porous structures at audible frequencies. *J. Acoust. Soc. Am.*, 102(4): 1995–2006, 1997.

<sup>11</sup> Limp materials have very low elastic modulus to mass density ratios. These properties can influence sound absorption properties. See e.g. F.-X. Bécot and F. Sgard. On the use of poroelastic materials for the control of the sound radiated by a cavity backed plate. *J. Acoust. Am.*, 120:2055–2066, 2006

<sup>12</sup> The shape factor is defined as the ratio between the sample volume and its free lateral surfaces.

<sup>13</sup> C. Langlois, R. Panneton, and N. Atalla. Polynomial relations for quasi-static mechanical characterization of isotropic poroelastic materials. *J. Acoust. Soc. Am.*, 110:3032–3040, 2001.





*Prepare to be MATELYS approved !*



**Prix Industrie 2012**



TMM-FTMM prediction tool



Micro-Macro models



Characterization assistant



ISO 10140 & 354 meas



In-duct sound meas & charac



Impedance tube meas



Material database



---

## MATELYS - RESEARCH LAB

Ltd liability company with total share 8250 euros  
*Agrément C.I.R. (Crédit Impôt Recherche) since 2007*  
*Déclaration d'activité de formation*  
*enregistrée n° 82691051869 auprès du préfet de Région*  
SIRET 487 596 009 00034 – TVA EU FR 06 487 596 009

Head office :  
7 rue des Maraîchers, Bâtiment B  
F-69120 VAULX-EN-VELIN  
Tél : +33 9 72 50 93 16 – Fax : +33 9 72 50 93 15  
<http://www.matelys.com> – [contact@matelys.com](mailto:contact@matelys.com)